WPJET1-CPR(17) 16889

A Huber et al.

The Near Infrared Imaging System for the Real-Time Protection of the JET ITER-like wall

Preprint of Paper to be submitted for publication in Proceeding of 16th International Conference on Plasma-Facing Materials and Components for Fusion Applications

This work has been carried out within the framework of the EUROfusion Consortium and has received funding from the Euratom research and training programme 2014-2018 under grant agreement No 633053. The views and opinions expressed herein do not necessarily reflect those of the European Commission.

The Near Infrared Imaging System for the Real-Time Protection of the JET ITER-like wall

A. Huber[1], D. Kinna[2], V. Huber[3], G. Arnoux[2], I .Balboa[2], C. Balorin[4], P. Carman[2], P. Carvalho[5], S. Collins[2], N. Conway[2], P. McCullen[2], S. Jachmich[4], M. Jouve[6], Ch. Linsmeier[1], B. Lomanowski[7], P. J. Lomas[2], C. G. Lowry[8,9], C.F. Maggi[2], G.F. Matthews[2], T. May-Smith[2], A. Meigs[2], Ph. Mertens[1], I. Nunes[5], M. Price[2], P. Puglia[10], V. Riccardo[2], F. G. Rimini[2], G. Sergienko[1], M. Tsalas[2], K-D. Zastrow[2] and JET contributors[#]

EUROfusion Consortium, JET, Culham Science Centre, Abingdon, OX14 3DB, UK

[1]*Forschungszentrum Jülich GmbH, Institut für Energie- und Klimaforschung – Plasmaphysik, Partner of the Trilateral Euregio Cluster (TEC), 52425 Jülich, Germany*
[2]*CCFE, Culham Science Centre, Abingdon, OX14 3DB, UK*
[3]*Forschungszentrum Jülich GmbH, Supercomputing Centre, 52425 Jülich, Germany*
[4]*Laboratory for Plasma Physics, ERM/KMS, B-1000 Brussels, Belgium*
[5]*Instituto de Plasmas e Fusão Nuclear, Instituto Superior Técnico, Universidade de Lisboa, Lisboa, Portugal*
[6]*CEA, IRFM, 13108 St Paul lez Durance, France*
[7]*Aalto University, P.O.Box 14100, FIN-00076 Aalto, Finland*
[8]*European Commission, B1049 Brussels, Belgium*
[9]*JET Exploitation Unit, Culham Science Centre, Abingdon OX14 3DB, UK*
[10]*Instituto de Física - Universidade de São Paulo Rua do Matão Travessa R Nr.187 CEP 05508-090 Cidade Universitária, São Paulo, Brasil*

E-mail: A.Huber@fz-juelich.de

Keywords: Imaging diagnostics, Real-Time protection system, Hot spots, JUVIL Software, Image processing

Abstract

This paper describes the design, implementation, and operation of the near infrared imaging diagnostic system of the JET-ILW plasma experiment and its integration into the existing JET protection architecture. Imaging systems contain four wide-angle views, four tangential divertor views, and two top views of the divertor covering 25%–66% of the main chamber wall and up to 43% of the divertor. The operation temperature ranges of NIR protection cameras for the materials used on JET are: Be 700-1400°C; W coating 700-1370°C; W 700-1400°C.
The Real-Time Protection system operates routinely since 2011 and successfully demonstrated its capability to avoid the overheating of the main chamber beryllium wall as well as of the divertor W and W-coated CFC tiles. During this period, less than 0.5% of the terminated discharges were aborted by a malfunction of the system. About 2-3% of the discharges were terminated due to the detection of actual hot spots.

1. Introduction

Plasma-Facing Components (PFC) in JET with the all metal Be/W ITER-like wall [1] are subjected to high heat fluxes which can lead to damages such as beryllium melting or thermal fatigue of tungsten. In order to safeguard the first wall of the JET machine, a protection system with real time control, based on imaging diagnostics, was implemented on JET in 2011/2012 [2,3]. It successfully demonstrated its capability to avoid the overheating of the main chamber beryllium wall as well as of the divertor W and W-coated tiles. The Vessel Thermal Map (VTM)

[#]See the author list of "Overview of the JET results in support to ITER" by X. Litaudon et al. to be published in Nuclear Fusion Special issue: overview and summary reports from the 26th Fusion Energy Conference (Kyoto, Japan, 17-22 October 2016)

combines temperatures of predefined Regions of Interest (ROIs) measured for diverse wall segments and raises alarms in response to overheating.
Considering the different materials on JET the real time imaging system must fulfil the following objectives:

- avoid the melting of the beryllium wall components (melting point of beryllium 1287ºC),
- minimize the risk of delamination of the tungsten coated tiles (the temperature should be kept below 1200ºC) [4]
- keep the surface temperature below the threshold at which the bulk tungsten re-crystallizes (1200ºC) [5],

These objectives require that the temperature monitoring of plasma-facing components (PFC) is considered mandatory for every plasma discharge in order to avoid overheating and eventual damage. Based on these purposes, protection cameras should deliver reliable measurements in the following operating temperature ranges for the main materials used on JET: Be 750-1400°C; W coating 750-1350°C; W bulk 750-1400°C. The required accuracy for the surface temperature measurement defined in the JET instructions is ±50ºC.

2. Feasibility of NIR Emission Measurements

Reliable measurements of the surface temperature are only possible when the background emission intensity is low. The registration of the thermal emission of the target could be contaminated with plasma bremsstrahlung emission, and emission due to the free-bound transitions (recombination).
Fig.1 shows the relative contributions of the continuum free-free, free-bound and thermal spectral radiance given a 2 m thick homogenous pure deuterium plasma.
The bremsstrahlung intensity as well as free-bound hydrogenic intensity was calculated using ADAS [6]. Plasma parameters for these estimates were chosen to determine typical high and low levels of Bremsstrahlung $P_{brem} \sim n_e^2 Z_{eff} T_e^{-1/2}$ [7]. The high density (10^{20}m^{-3}), low

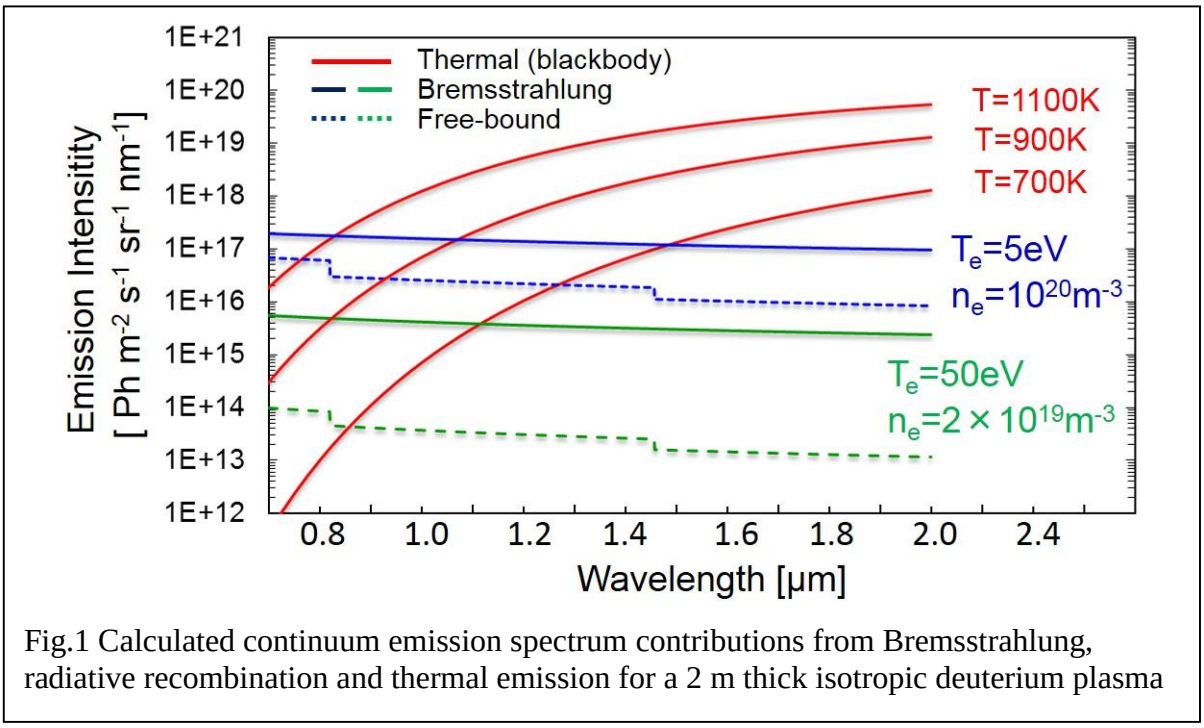

Fig.1 Calculated continuum emission spectrum contributions from Bremsstrahlung, radiative recombination and thermal emission for a 2 m thick isotropic deuterium plasma

electron temperature case (T_e=5eV), represents the detached plasma conditions and low density (2×10^{19}m^{-3}) and high electron temperature (T_e=50eV) are typical parameters for the attached divertor on JET.

The thermal emission was calculated using Planck's blackbody emissivity formula for three surface temperatures, 700K, 900K and 1100K. The free-bound emission intensity is low and can generally be neglected. The bremsstrahlung emission starts competing with thermal emission only at very high densities, high Z_{eff} levels and surface temperatures below 1000K. For temperatures in excess of 1000K the thermal emission will dominate in the NIR spectral range. The lower limit for temperature measurement with NIR systems is thus around 1000K, fulfilling the requirement for protection systems at JET.

3. The Near Infrared Imaging System on JET

3.1 Protection Cameras

For reliable operation of the imaging system in the hostile electromagnetic environment of JET, the protection cameras must meet the following main criteria: non-disturbed operation of CCD sensors and electronics in the presence of a magnetic field and they should have an acceptable resistance to neutrons and gamma radiations. Video cameras should operate without replacement at least one year, withstanding the neutron fluence of ~2×10^{12} n/cm^2 [8]. In contrast to the digital video camera the analogue one could fulfil this criteria easily because of its robustness and stable operation under harsh electromagnetic conditions – features which are particularly desirable in protection systems. The drawback of this pragmatic choice is the rather low sensitivity around 1μm wavelength (<10%) for silicon-based detectors and the low dynamic range (8bit).

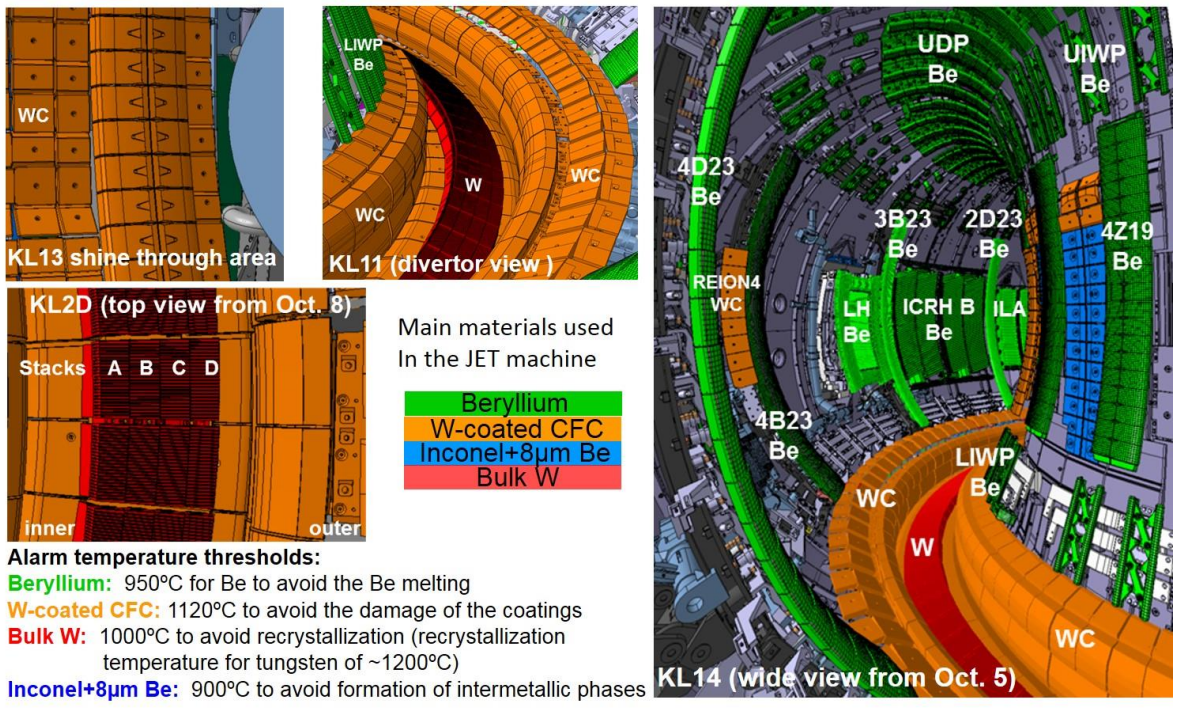

Fig.2 Fields of View (FoV) of protection NIR CCD cameras

The JET imaging system for machine protection is based on analog monochrome CCD cameras (Hitachi KP-M1AP; sensor: Sony ICX423AL, Sensor size 768x576, pixel size: 11.6 μm (H)×11.2 μm (V) [9]), equipped with near infrared (NIR) filters. Based on analysis of the NIR spectra, two types of band pass filters have been used: 980±10 nm and 1016±40 nm. Synchronized with the external sync signals (V/H scans) the cameras operate in non-interlaced mode at 50 fields per second with binning (odd and even lines are exposed together at the same time). In this mode, the spatial resolution is lost in the vertical direction: the camera delivers images with an apparent size of 720×288 pixels every 20ms. At the same time, the pixels are effectively larger in the vertical direction, and hence more sensitive.

Imaging systems contain four wide angle views, four tangential divertor views, two top views of the divertor, and one view of the NBI shine through area covering 25%–66% of the main chamber wall and up to 43% of the divertor.

The calibration of the imaging system with high accuracy has been performed with the help of an in-vessel radiometric light source which has been brought inside the JET vacuum vessel by means of the remote-handling arm [10]. As a result of the calibration, the operation temperature ranges for the materials used on JET are Be 650-1600ºC, W coatings 600-1320ºC, and W bulk 650-1500ºC.

Figure 2 shows examples of typical field of views of different imaging system on JET with ITER like wall. Different colours represent the different materials of the first walls used on JET: green – beryllium; red –bulk tungsten; orange –W-coated CFC; blue – Inconel coated with 8µm Be. The solid tungsten tile appears dark orange or even dark grey on some figures owing to the numerous lamellae and viewing angle in the picture. The most important components the temperature of which should be routinely monitored are the beryllium inner and outer limiter, bulk tungsten in the divertor (Tile 5) and the W-coated horizontal and vertical divertor CFC tiles.
The typical alarm temperature thresholds used for the real-time protection of the first wall on JET are:

- **Beryllium:** 950ºC for Be to avoid the Be melting
- **W-coated CFC:** 1120ºC to avoid the damage of the coatings
- **Bulk W:** 1000ºC to avoid recrystallization (recrystallization temperature for tungsten of ~1200ºC)
- **Inconel+8µm Be:** 900ºC to avoid formation of intermetallic phases [11].

3.2 Spectral emissivity of JET materials

The JET main chamber is protected by guard limiters covered with castellated beryllium tiles. Furthermore, the divertor horizontal targets are constituted of bulk tungsten lamellas whereas the vertical targets are CFC coated tiles with a 12-20µm tungsten layer. For surface temperature measurements with high accuracy, as required for the JET wall protection, the knowledge of the spectral emissivity of each material in use is essential.
The tungsten spectral emissivity, shown in Fig.3 for different surface temperatures, is well documented [12]. The so-called "X-point of W", where the emissivity wavelength isotherms cross, corresponds to λ≈1.27 µm. The usage of the cameras equipped with IFs at the central wavelengths of 980nm and 1016nm, close to the "X-point," brings the advantage of a weak

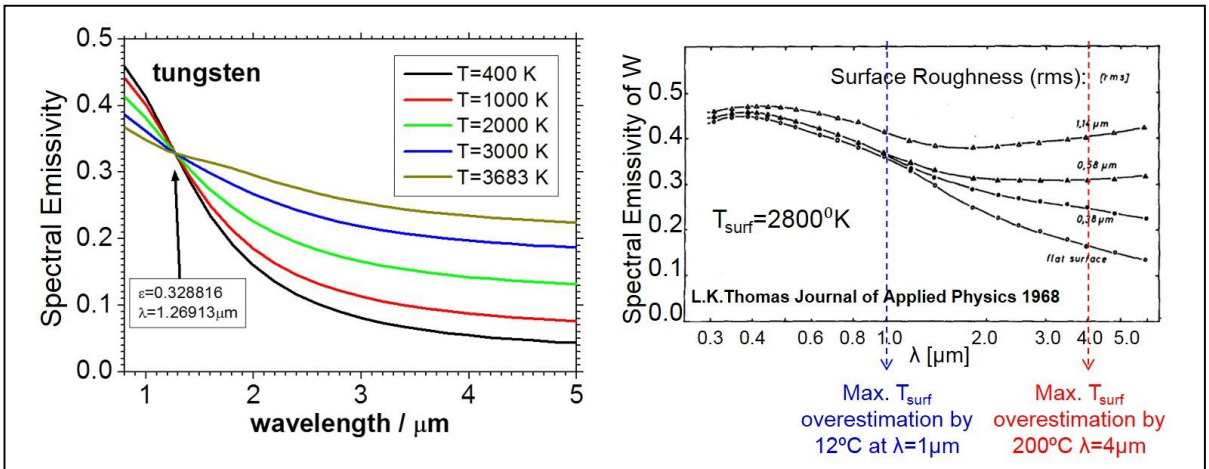

Fig. 3. (left) W spectral emissivity according to [12] and (right) the normal spectral emissivity of W with different surface roughness in dependence of wavelength [14].

dependence of ε_λ on temperature. The emissivity of the W coatings deposited on Dunlop DMS 780 was investigated in the range of 700 –1200°C [13] using a steady state heating regime. A value of 0.63±0.07 at λ=1064 nm was found for 10μm thickness, while for 20 μm the spectral emissivity was 0.59±0.06. This spread of values is due to the structure of the CFC substrate. In the temperature range 700–1200°C, there is no significant dependence of the W coating emissivity on the surface temperature at λ=1.064 μm. At higher wavelengths, though (measured at 1.75 μm and 4 μm), the emissivity increases with the temperature. No significant change of the emissivity after plasma exposure in JET (experimental campaigns in 2011-2012) was detected for the vertical W-coated CFC Tiles 3, 4 and 7 [13].
Additionally, beryllium emissivity measurements have been performed on the JET neutral beam test bed. The values of emissivity used for the protection NIR imaging cameras (with IF 1016 ± 40 nm) are: bulk tungsten $\varepsilon=0.42–1.98\times10^{-5}\times T$ (K); W coatings ε=0.6; beryllium ε=0.25.

The surface roughness could have a significant impact on the emissivity of the object [14]. As shown in [14] and in the figure 3 the surface roughness (rms) of about 1μm could lead to the increase of spectral emissivity by the value of $\Delta\varepsilon \approx 0.02 - 0.05$ at λ=1μm. In the MWIR wavelength range the impact of the surface roughness onto the spectral emissivity is even stronger: for example the surface roughness of 0.38μm (1μm) leads to increase the emissivity from 0.16 to 0.24 (0.4) at λ=4μm and at surface temperature of 2800ºK. For NIR measurements of surface temperatures around 1000ºC, such a roughness provokes a relatively small emissivity uncertainty of $\frac{\Delta\varepsilon}{\varepsilon}\sim0.02 - 0.05$ leading to a maximal temperature overestimation by 12ºC. In contrast to NIR measurements, the MWIR and LWIR detection is much strongly impacted by the surface roughness due to the fact of the smaller emissivity values at longer wavelengths: the emissivity inaccuracies are $\frac{\Delta\varepsilon}{\varepsilon}\sim0.50 - 1.0$ for the MWIR method for the expecting surface roughness 0.38-1.0 μm. Such larger uncertainties on the emissivity could lead to the significant overestimation of the surface temperature. For example, the MWIR method with accuracy of $\frac{\Delta\varepsilon}{\varepsilon}\sim0.50$ will overestimate T_{surf} by the value of 200ºC during the measurements in the temperature range around 1000ºC, thus infringing the requirements of the accuracy measurements (±50ºC) by the real-time protection system.

3.3. Video Digitization and distribution

A data flow diagram which includes fundamental hardware components is shown in Fig.4. The video input is an analogue composite video signal. This signal will be digitised by a Gigabit Ethernet (GigE) frame grabber. The frame grabber sends the data using networking technology to three separate destinations simultaneously [15]: the Real Time Processing System, a Video Capture and replay system for data storage, and the systems running the live displays. This setup is repeated for each Hitachi camera.

The frame grabber is the Pleora iPORT PT1000-ANL (2-6-V2-E). It takes a composite video feed and generates a stream of packets of video data on a GigE network connection.
The iPORT is also capable, in conjunction with a suitable network switch, of sending its data to multiple destinations without sending duplicate frames of data to each. Cameras act as temperature sensors: pixel intensities are calibrated to temperature. Each camera monitors multiple regions of interest (ROIs) for their maximum temperature. A real time processing unit (**RTPU**) system [16] has to be capable of handling a maximum of 96 ROIs per camera. It calculates the temperature for each camera and sends the result across JET's Real Time Data Network (RTDN) to a separate real time system, the Vessel Thermal Map (**VTM**) [17,18]. The Vessel Thermal Map assimilates all temperature inputs and, using the knowledge of how camera ROIs map to physical components, identifies **Events.** If the temperature from an active ROI of some camera crosses a threshold (which will trigger the alarm), the VTM

communicates to the Real Time Protection Sequencer (**RTPS**), which decides how the control

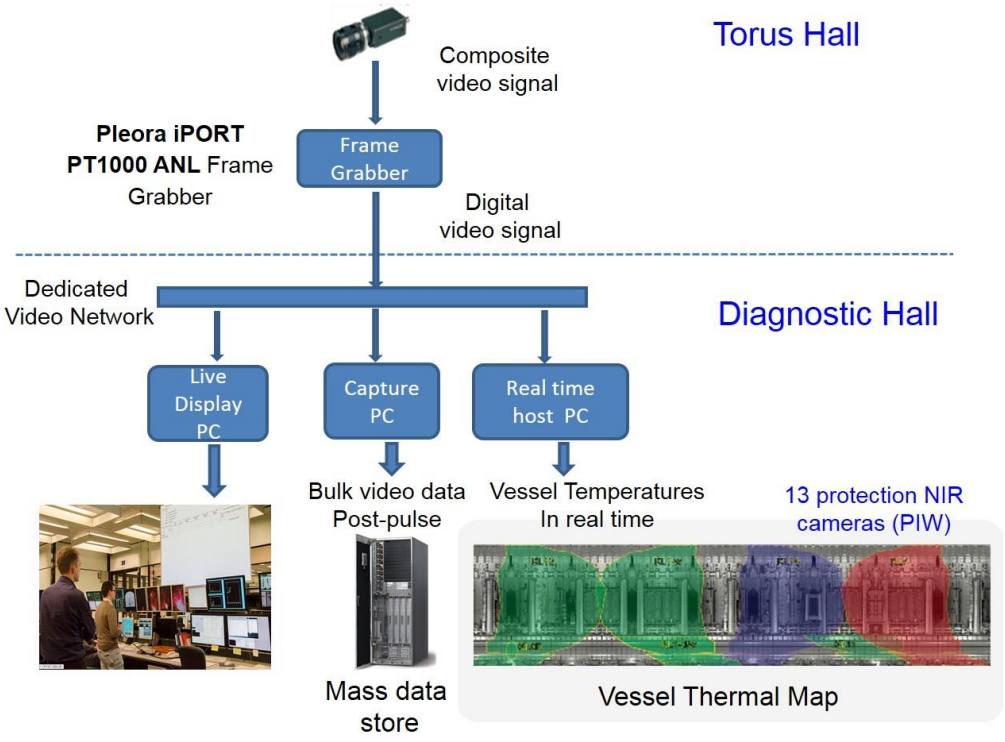

Fig.4 Video digitization and distribution synoptic.

actuators should respond. The response of the RTPS is programmable.

The RTPU is a field programmable gate array (FPGA) board that performs the real time image processing. The chosen FPGA board is a "Sundance Multiprocessor" PCI express SMT122T FX70T board. The main functions of the real time processing algorithm are:

- to evaluate the temperatures of multiple ROIs on each image of the video stream.
- to ignore 'dead' pixels with artificially high or low intensity
- it can apply a median filter and a per-pixel correction for sensor irregularities. False hot spots due to neutron hits on the sensor are discarded by using a median filter. The other false hot spots, due for example to dust deposits, are eliminated by using a selection algorithm. This algorithm ignores hot spots that are too small. A dynamic ROI of 5 × 5 pixels is defined around the hottest pixel. If the minimum number of pixels, *N*pix, above a threshold (in percent of the value of the hottest pixel) is found, the hot spot is considered valid. If not, the next hottest spot is selected and the validation process is repeated. *N*pix and the threshold are configurable parameters. We use typically: *N*pix=5 and a threshold of 90%.
- Calibration is done using a look-up table for the material that the ROI is known to be observing.

3.4 Software Framework for Data Analysis of JET Imaging Systems

A new powerful software framework JUVIL (JET Users Video Imaging Library) [19] has been developed and successfully installed at JET for fast data visualization and advanced analysis of all types of imaging data. The JUVIL framework is based on modular object-oriented components implemented in Python to simplify work with JET scientific data. It provides standard interfaces to access video data and post-processing, which are highly configurable and can be easily extended and adapted for new data formats and imaging cameras. JUVIL contains a Logbook Editor, which loads automatically the raised VTM events as well as the alarms during an arbitrary pulse and stores them to the logbook. Additionally, a specifically

developed Hotspot Editor is recognized as an excellent tool for the investigation of the formation and development of hot spots and for their evaluation [20].

4. The Real-Time Protection System in Action

The surface of the JET-divertor is protected against melting by six video imaging cameras, four with tangential divertor views, and two top views of the divertor (see field of views in Fig. 2). These protection cameras with divertor views cover the following temperature ranges: W coating CFC tiles 700-1370°C and bulk W 700-1400°C. The divertor tiles are chamfered in toroidal direction to avoid leading edges (the so-called shadowing). Nevertheless, damages of the tungsten coatings or bulk tungsten tiles can happen in the high heating power plasma pulses. Fig.5 shows an example for a discharge with a classical heat up of the divertor W tiles. The outer strike point of this plasma discharge is located on the bulk tungsten Tile 5. This pulse was a typical ELMy H-mode plasma with auxiliary heating power of ≈12MW (P_{NBI}=9.6MW and

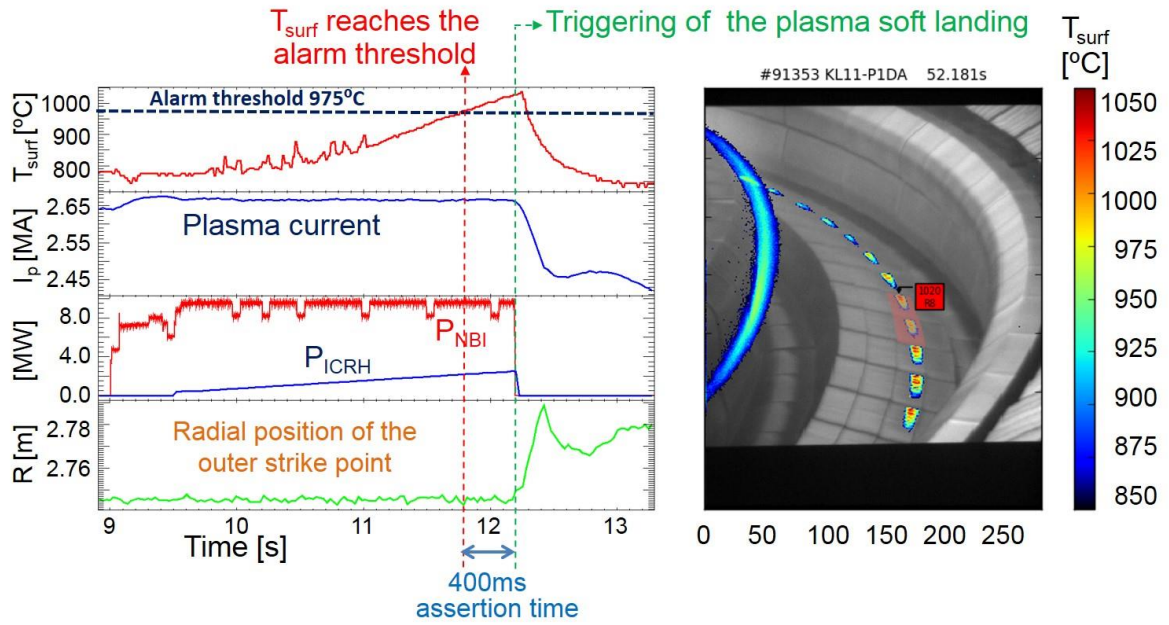

Fig.5 A discharge with a classical heat up of the divertor W bulk tiles.

P_{ICRH}=1.0-2.5MW). The surface temperature increases during the auxiliary heating phase with time. At time 11.8s the surface temperature of the bulk tungsten tile reaches the trip level of 975°C and remains above this trip level for longer than the assertion time, which is 400ms. At time 12.2s VTM sends an alarm to RTPS requesting an appropriate action from the plasma control systems. As a result the plasma was carefully terminated by switching of the auxiliary power, moving the strike points away and ramping down the plasma current. The "assertion time" is the time window during which VTM checks that the temperature of the analyzed surface is consistently above the trip level. This is needed to avoid false alarms due to spurious signals on the camera image (e.g. caused by neutron impact). During the response time of the plasma control systems after receiving the tripping level, the temperature still increases and reaches the maximal value of 1030C that is significantly below the threshold at which the bulk tungsten re-crystallizes (1200°C).

5. VTM Alarm statistics

On JET, every plasma termination due to VTM alarms requires prompt careful analysis of the reason of the plasma stopping by viewing operator (VSO). In order to provide a fast data visualization and advanced analysis of all types of VTM alarms, a new software *VSO Logbook*

Editor [19] has been developed and successfully installed at JET. Thanks to this tool, all VTM alarms on the JET machine are well characterised and catalogued. An analysis of the reasons for early termination of the plasma pulses is shown in Figure 6. Directly after implementation of the protection system on JET during the campaigns C31, C32 and C33, the statistics showed a large number of the VTM alarms due the classical heat up of the first wall components, to hot spots formation and to the heating by NBI beam re-ionization. The latter are the hot loads on

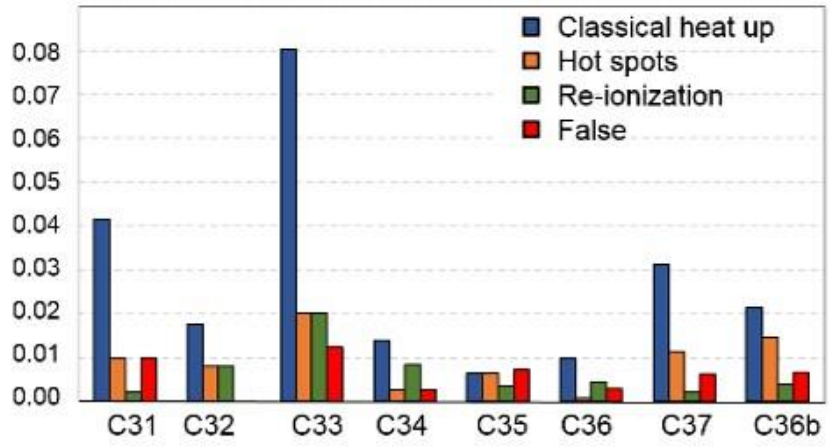

Fig. 6 Number of VTM alarms per campaign normalized to the number of total campaign shots.

the limiter subjected to the impact of the re-ionised neutrals injected by the heating system. During the C33 campaign, about 8% of the plasma discharges were terminated by RTPS to avoid harmful situations like dangerous overheating through classical heat up of the wall components. Also the number of hot spots (2% of the plasma pulses) as well as the alarms due the NBI beam re-ionization (2%) increased. The following campaigns C34-C36 show a general tendency of reduction of the VTM alarms because of the continuous improvement of the real-time protection system as well as a better understanding of the physics of the alarm reasons. Within the last experimental campaigns (C37 and C36b) a significant improvement of the auxiliary heating systems on JET has been performed leading to a marginal increase of the plasma terminations due to RTPS safety system: about 2-3% due to the classical heat up and about 1-1.5% due to the hot spot formation. As the statistics show, despite the JET heating power improvement false alarms could be reduced to less than 0.5% of all plasma discharges.

Conclusion

The ITER-like Wall protection system based on video imaging was developed on JET and is reliably operated. Safe landing of the plasma is achieved when hot spots are observed on the Be main chamber as well as in the divertor PFCs (bulk W and tungsten coated CFC tiles).

Composed with a set of 13 CCD cameras, the protection system is based on one commercial FPGA board per camera. In the proposed approach, each FPGA board can manage up to 96 ROIs whilst for each ROI the value and position of the hottest pixel are delivered and sent to JET's VTM (Vessel Thermal Map). The NIR wavelength range is a good choice for temperature monitoring (T>1000ºK) fulfilling the requirements of the accuracy measurements (±50ºC) by the real-time protection system.

A hot spot validation algorithm was successfully integrated into the real-time system and is now used to avoid alarms caused by false hot spots.

The real-time video imaging system has been operated routinely over 12000 discharges since 2011. According to the JET operation instructions no plasma discharge could be started without this protection system. It was demonstrated that the video imaging protection system can work properly under harsh conditions with neutrons and dust on the surface as well as layer deposits

on the materials. Within the last experimental campaigns 2-3% of the plasma discharges were terminated by RTPS to avoid harmful situations like dangerous overheating. The different detection algorithms fulfil their tasks reliably. False positive alarms could be reduced to less than 0.5% of all plasma discharges.

Acknowledgements

This work has been carried out within the framework of the EUROfusion Consortium and has received funding from the Euratom research and training programme 2014-2018 under grant agreement No 633053. The views and opinions expressed herein do not necessarily reflect those of the European Commission.

References

[1] G. F. Matthews et al., Phys. Scr.T145 (2011) 014001 (6pp)
[2] G. Arnoux et al., Rev. Sci. Instrum. 83, 10D727 (2012)
[3] A. Huber et al., Rev. Sci. Instrum. 83, 10D511 (2012)
[4] H. Maier et al., Phys. Scr. T138 (2009) 014031 (5pp)
[5] Ph. Mertens et al., Phys. Scr. T138 (2009) 014032 (5pp)
[6] Summers H.P. Atomic Data and Analysis Structure, URL: http://www.adas.ac.uk/
[7] A. T. Ramsey and S. L. Turner, Rev. Sci. Instrum. 58, (1987) 1211.
[8] A. Huber et al., Fusion Eng. Des. (2017),
http://dx.doi.org/10.1016/j.fusengdes.2017.03.167
[9] http://www.eureca.de/english/optoelectronics_sony.html
[10] V. Huber, A. Huber, D. Kinna *et al.*, Rev. Sci. Instrum., **87**, 11D430 (2016); doi: 10.1063/1.4959912
[11] T. Hirai et al., Physica Scripta, T128, 166 (2007).
[12] CRC Handbook of Chemistry and Physics, 75th ed., edited by D. R. Lide and H. P. R. Frederikse (CRC, 1994).
[13] C. Ruset et al., *Preprint*, JW10-TA-PIW-ACIR-02 (2012).
[14] L. K. Thomas Journal of Applied Physics (1968) **39,** 4681-4686.
[15] D. Kinna, JET CDN Report H(10)007 (2010)
[16] M. Jouve, et al., Real-time protection of the ITER-like wall at JET, in: Proc.13th Int. Conf. on Accelerator and Large Experimental Physics Control Systems, Grenoble, 2011.
[17] A. Stephen, et al., Centralised coordinated control to protect the JET ITER-likewall, in: Proc. 13th Int. Conf. on Accelerator and Large Experimental Physics Control Systems, Grenoble, 2011.
[18] D. Alves et al., Phys. Rev. ST Accel. Beams 15 (2012)
[19] V. Huber, A. Huber, D. Kinna et al., Fusion Eng. Des. (2017),
http://dx.doi.org/10.1016/j.fusengdes.2017.03.005
[20] V. Huber et al., this conference